Lasers in Manufacturing Conference 2015

Correlation of keyhole dynamics and pore formation

J. Volpp[a]*, F.Vollertsen[a,b]

[a]BIAS – Bremer Institut für angewandte Strahltechnik GmbH, Klagenfurter Straße 2, 28359 Bremen, Germany
[b]University of Bremen, Germany

Abstract

Imperfections like pores occurring due to high process dynamics during laser deep penetration welding reduce the weld quality and the strength of welded joints. It is assumed that keyhole instabilities are responsible for the high process dynamics. In order to better understand the correlation between pore formation and keyhole dynamics an analytical process model has been developed describing keyhole radius fluctuations in different depths depending on the process parameters. Modelled radius oscillation frequencies have been compared to experimentally measured process emissions. Frequency spectrums of acoustic process emission observations show similar tendencies of keyhole dynamics compared to the calculations. For pore detection x-ray photography has been used while pore percentage and pore number in the weld seams have been evaluated. The pore formation in the solidified weld seam is compared to the observed dynamic characteristics during the process. Higher keyhole frequencies tend to correlate with increased pore numbers at reduced pore sizes.

Keywords: Laser deep penetration welding; Keyhole dynamics; Acoustic process emission, Pore formation

1. Introduction

In order to understand the laser keyhole welding process several physical effects have to be considered. The laser beam interacts with the material depending on e.g. the penetration angle or the wavelength of the beam [1]. Multiple reflections of the beam in the keyhole change the energy deposition which affects the local temperatures and ablation rates [1]. Ablation results in vapor creation in the keyhole and pressure which keeps, on the one hand, the keyhole open against the surface tension pressure of the surrounding melt pool [2]. On the other hand, vapor and inhomogeneous energy distribution on the keyhole wall, which can be

* Corresponding author. Tel: +49 421-218-58135; fax: +49 421-218-58063.
E-mail address: Volpp@bias.de.

introduced by fluctuations of the laser intensity [3] or laser power variations from the laser machine [4], can lead to occurring dynamics during the process [5]. These dynamics can be radius and depth variations of the keyhole. Klein et al. [6] described three possible keyhole deviations: radial, azimuthal and axial. In addition, the keyhole varies in depth, visible in the keyhole depth measurement [7], and produces spiking [8]. These instabilities seem to be a possible reason for imperfections in the process like process pores that reduce seam quality. Process pores are formed due to either keyhole collapses or bulging of the keyhole and immediate collapse of the bulging due to sudden condensation [9]. Both possible mechanisms should result in characteristic temporal keyhole movement. Attempts were done in order to measure this dynamic keyhole behavior. A high speed camera has been used to record keyhole opening fluctuations [10]. Unfortunately, this method gives no direct information about the keyhole behavior inside the keyhole. However, some of this information is transferred to the keyhole opening by the vapor fluctuations induced inside the keyhole. High speed x-ray imaging can show the keyhole and its behavior during the process [11] but keyhole dynamics are not visible with current systems due to low resolution and recording frequency. Sandwich methods that use transparent material like glass in front of the welded material provide the possibility to visualize the keyhole during welding at high recording frequencies using high speed cameras [12]. However, different material properties of the glass and metal influence the process. For indirect measurement of process dynamics, laser back reflections from the process can be used. Oscillating melt pool surfaces or keyhole radii in the process lead to oscillating reflections of the laser beam which can be recorded using photo diodes. Geiger et al. [13] used a Silicon-diode capturing light from the visible spectrum up to the laser wavelength. Frequencies from 100 Hz to 600 Hz have been related to the melt pool and frequencies higher than 1 kHz to the keyhole fluctuations. Acoustic emissions can be also used for detecting characteristic keyhole behavior. Dynamic radii and vapor pressure oscillations in the keyhole induce sound waves that can be recorded by a microphone. Hoffmann et al. [14] found that keyhole oscillations during welding with a CO_2 laser take place in the range of 0.8 kHz to 4 kHz. Fabbro et al. [15] observed the vapor plume in order to indirectly measure pressure changes inside the keyhole as there is a relation of exiting vapor through the keyhole opening and the dynamics inside the keyhole. Dynamic measurements based on this method observed process frequencies from 0.7 kHz to 5 kHz [16].

Modeling has been used to get a better insight into the process due to challenges of visualizing the keyhole welding process during experiments. Numerical models provide detailed information about the process [17], but calculation times are typically very high [18]. Dynamic modeling with numerical simulation found keyhole oscillations at frequencies higher than 3 kHz [19]. Analytical models need more simplifications but calculation time is much lower. Kroos et al. [2] and Klein et al. [20] created an analytical, self-consistent model of the keyhole. The model is based on a solution of the energy equation to obtain the surface temperature of the keyhole that is needed for the pressure equation to calculate the keyhole radius. Simplifications concerning keyhole shape, for which a solution of the heat conduction equation is known, are necessary. Thus, complete penetration of thin sheets is assumed. Radial oscillation frequencies have been calculated to 1.5 kHz [6].

Based on existing models an analytical model for deep penetration laser welding is used in this work in order to calculate the dynamic keyhole behavior. Experimental evaluation is conducted using acoustic process monitoring. Measured and experimentally determined dynamic characteristics of the keyhole are correlated to the pores found in x-ray imaging after the process.

2. Methods

For the experiments, two lasers have been used, an IPG fiber laser (YLR8000S) providing a Tophat intensity distribution (Fig. 1a) in the focal layer and a Trumpf rod laser (HL4006D) having a Gaussian-like intensity profile in the focal layer (Fig. 1b). The spot diameter for both setups is measured to 0.56 mm. Besides beam profile variation, welding velocity is varied from 1.5 m/min to 3 m/min.

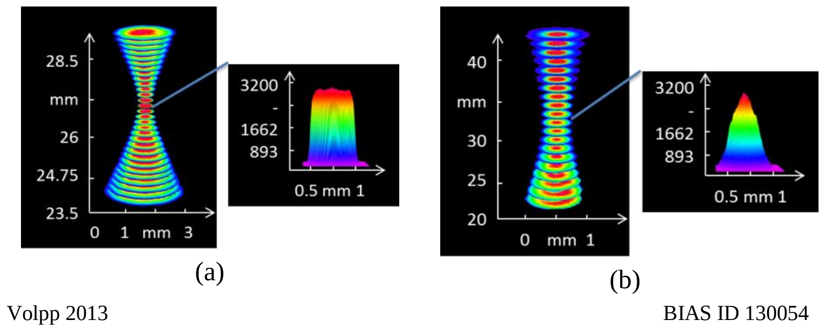

Figure 1. Measured intensity profiles along the beam axis and intensity distribution in the focal layer for (a) IPG fiber laser (YLR8000S) and (b) Trumpf rod laser (HL4006D) [21]

Acoustic emissions are recorded during welding using a microphone (Mc Crypt Microphone Mc-87 Pro, sensitivity: 60-15000 Hz) and a transient recorder that records the acoustic signal at a recording frequency of 50 kHz. The recorded time signal of 2 s length is transferred to its frequency spectrum using Fast Fourier Transformation. Pore number and pore percentage in the weld seam are measured for each welded specimen in x-ray images. X-ray images are taken as shown in Figure 2a. A representative seam of 30 mm length is taken for evaluation (Figure 2b). Pore number, pore area and weld seam area are identified from the images using Matlab (Version R2009a). The ratio of pore and seam area is taken for the pore percentage calculation.

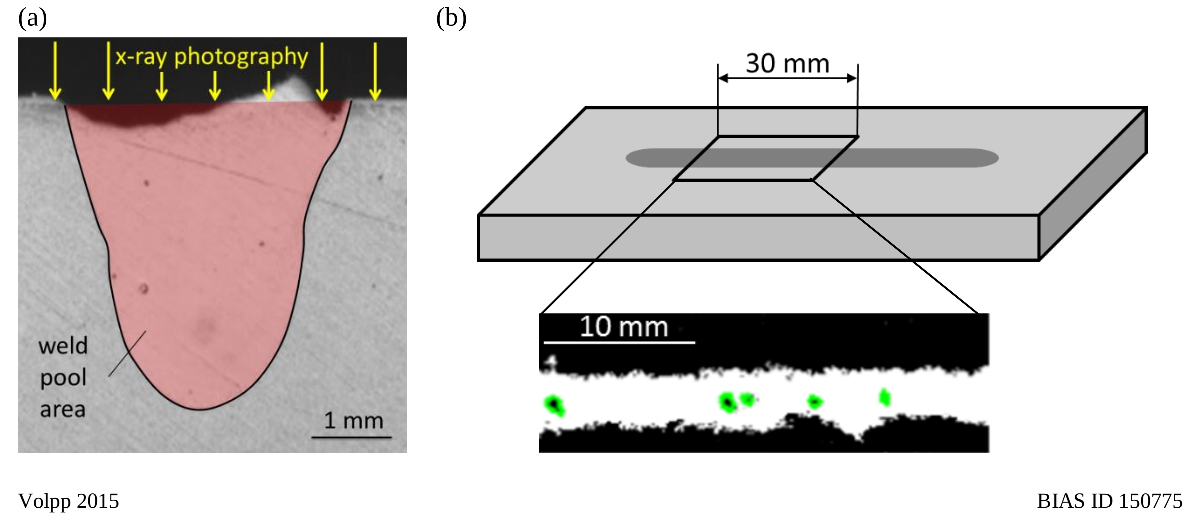

Fig. 2. (a) Cross section polish (4 kW laser power, 1.5 m/min welding speed, Gaussian-like profile, EN AW 6082) [22]; (b) sketch of a specimen and an exemplary processed x-ray image for seam and pore detection

Modeling of keyhole parameters is conducted. An analytical process model is used based on the models of Kroos et al. [2] and Klein et al. [20]. Quasi-static keyhole radii and pressures are calculated in different sections in depth of the keyhole by solving the pressure balance equations consisting of the ablation pressure working against the surface tension pressure of the surrounding melt pool [23]. Dynamics are calculated by solving differential equations describing the pressure and radius oscillations in all sections in depth [24]. Calculation results give characteristic keyhole radius oscillation frequencies and amplitudes for each calculated section in depth of the keyhole.

Calculated and measured keyhole oscillation frequencies are compared to validate calculated results of the model. In addition, the model provides information about the radii of the keyhole and amplitudes of its oscillations which cannot be measured experimentally.

3. Results

Acoustic measurements and analytical keyhole modeling have been conducted for different parameter sets. The spectrum is analyzed by detecting dominant peaks in the frequency spectrum. In the vicinity (300 Hz to smaller and 300 Hz to higher values) of each frequency step in the spectrum the maximum frequency value is determined. If the frequency value is higher than the average frequency of the observed range it is considered a dominant peak. Dominant peaks are marked in the frequency spectrums of the acoustic measurements (Figure 3).

At different beam profiles the peaks appear at different frequencies. The main peaks for the Gaussian-like beam profile appear at lower frequencies compared to the spectrum of the Tophat profile (Figure 3). Most significant frequencies in the spectrum of the Gaussian-like beam process appear at 2800 Hz, at 4500 Hz 6200 Hz and at 9000 Hz at all evaluated welding velocities. In the spectrum of the Tophat beam process most significant frequencies are 5600 Hz, around 10 000 Hz, 11 200 Hz and up to 13 500 Hz.

When changing the welding velocity from 1.5 m/min to 3 m/min (Figure 3) the frequency spectrums change. Amplitudes slightly decrease in general at increasing welding velocity. At higher welding velocities the amplitudes of the peaks at high frequencies become more dominant compared to the amplitudes of the lower frequencies. These effects are more dominant when using the Tophat beam.

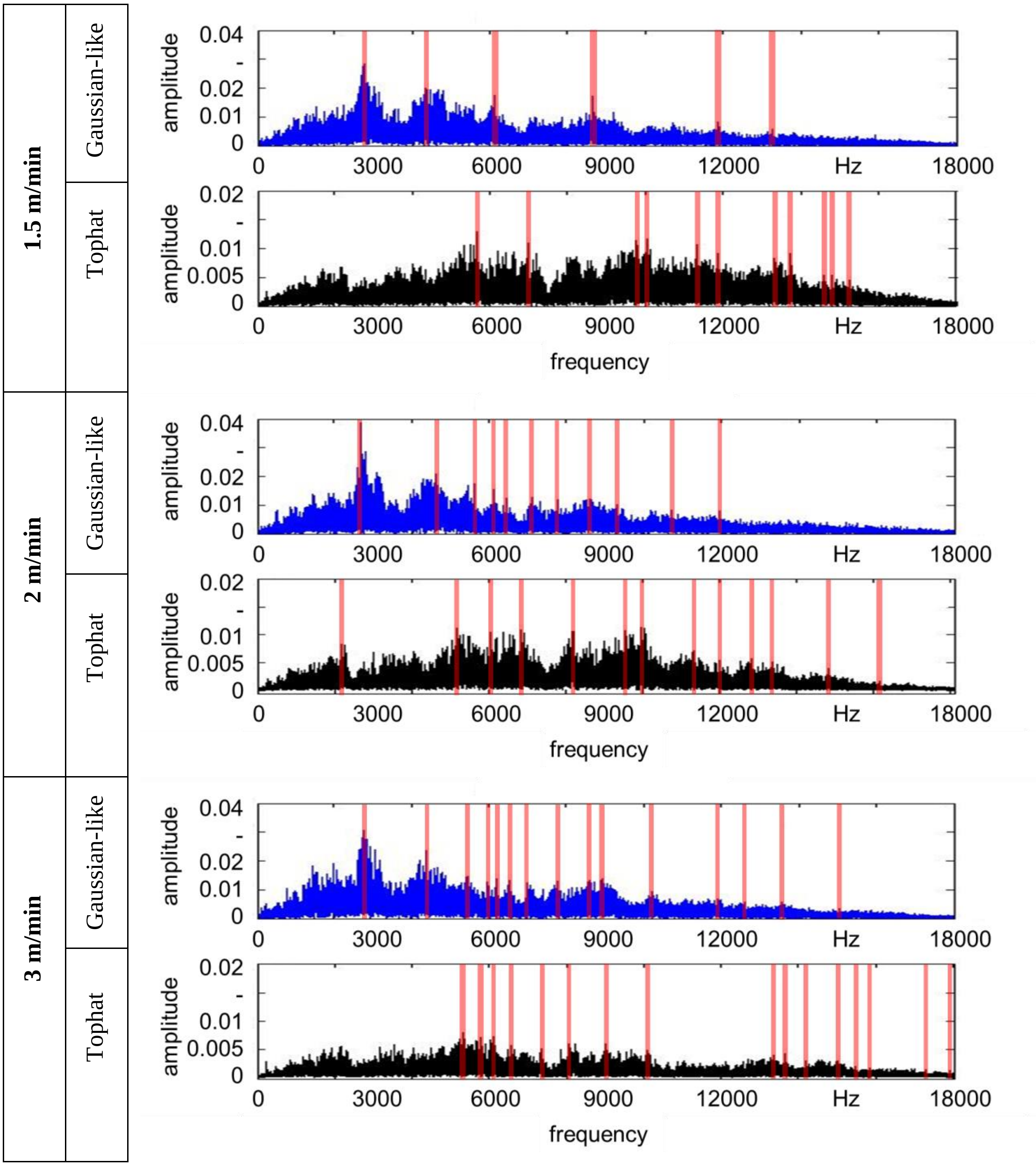

Volpp 2015

BIAS-ID 150776

Figure 3. Frequency spectrums of acoustic process emission measurements (Gaussian-like and Tophat beam at 0.56 mm spot size, 4 kW laser power, 50 kHz recording frequency, 2 s recording time) including frequency peaks in the spectrum (red lines) evaluated by determining frequency maximums in the vicinity of ±300 Hz around each frequency step

For the analysis of modeled results frequencies and amplitudes of all sections are taken. The average, the maximum and minimum are calculated and printed in Figure 4. Higher average and maximum frequencies are visible for a Tophat beam profile compared to a Gaussian beam, except for 1.5 m/min welding velocity (Figure 4a). Frequencies decrease at higher welding velocities when using a Gaussian beam profile. Amplitudes decrease at increasing velocity for both profiles, while amplitudes always show higher absolute values for a Gaussian beam profile (Figure 4b).

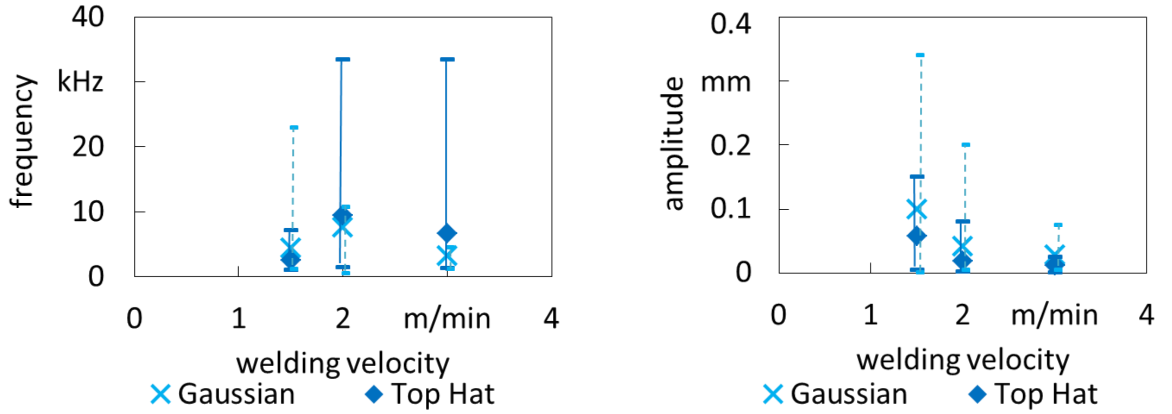

(a) (b)

Volpp 2015 BIAS ID 150777

Figure 4. Modelled frequency spectrums of Gaussian and Tophat beam keyhole oscillations (a) and modelled amplitudes of process oscillation (b) during the welding process at varied welding velocity (4 kW laser power, EN AW 6082 base material)

X-ray imaging of the weld seams of the specimens are used for pore identification as well as pore and seam area measurement. Pore number and pore percentage are determined at different welding velocities and beam profiles (Figure 5). Pore number is equal or lower in case of a Gaussian profile for all specimens (Figure 5a) while pore percentage is always higher compared to the Tophat profile (Figure 5b).

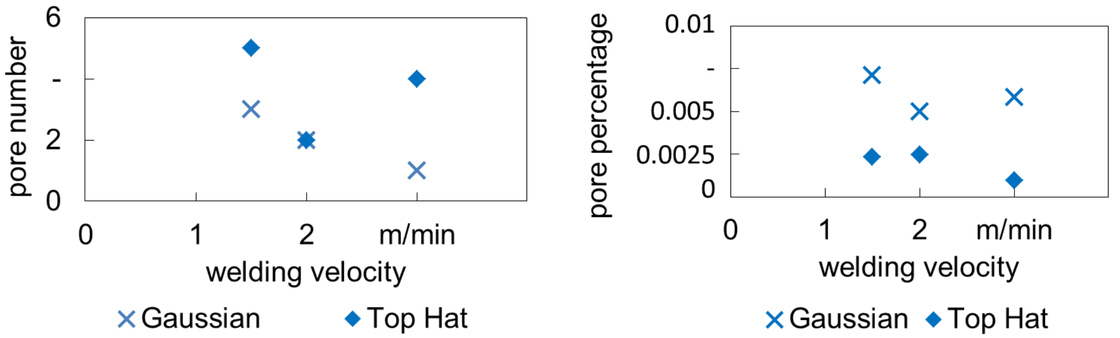

(a) (b)

Volpp 2015 BIAS ID 150778

Figure 5. Pore number (a) and pore percentage (b) at different welding velocities and beam profiles (4 kW laser power, EN AW 6082 base material)

4. Discussion

Calculations show the tendency of higher frequencies and lower amplitudes produced by the Tophat profile of the laser beam compared to a Gaussian profile which is in agreement with the experimentally measured spectrums. In the acoustic measurements a relative increase of amplitudes at higher frequencies compared to amplitudes at lower frequencies can be seen at increasing welding velocity for both profiles. This effect is more pronounced in case of the Tophat profile. This observation is in agreement with the tendencies of the modeled results. The general decrease of amplitude values at higher welding velocities can be seen in experiments, especially at Tophat welding, and in the model. The model seems to predict the correct tendencies of dynamic values in the process in the observed range of varied parameters. The modeled dynamic keyhole parameters are compared to the seam porosity in order to find correlations. For a Gaussian-like profile lower frequencies and amplitudes lead to a lower pore number and lower pore percentage. For both profiles, high frequencies tend to correlate to a tendency to a higher pore numbers, while the amplitudes seem to mainly determine the size of the pores and therefore the pore percentage. The lowest pore percentage can be achieved when using a Tophat beam at high welding velocity in this study where low amplitudes are present. The high frequencies at this parameter set seem to cause the high pore number.

5. Conclusions

Based on the present results, it can be concluded that the keyhole dynamics and the pore formation can be influenced by the focal beam profile. The comparison of porosity and acoustic measurements to modeled keyhole dynamics revealed that frequencies seem to correlate to the pore number while keyhole amplitudes influence the pore percentage. High frequencies at low amplitudes correlate with high pore number and low pore percentage.

Acknowledgements

This work was accomplished within the Center of Competence for Welding of Aluminum Alloys (Centr-Al). Funding by the DFG (VO 530/52-2) is gratefully acknowledged.

References

[1] Dausinger, F.; Strahlwerkzeug Laser: Energieeinkopplung und Prozesseffektivität. Teubner, Stuttgart, 1995.
[2] Kroos, J.; Gratzke, U.; Simon, G.: Towards a self-consistent model of the keyhole in penetration laser beam welding. In: J. Phys. D: Appl. Phys. 26 (1993) 474-480.
[3] Khan, M.;Romoli, L.; Dini, G.; Fiaschi, M.: A simplified energy-based model for laser welding of ferritic stainless steels in overlap configurations. CIRP Annals, E, 60/1/2011, P.215.
[4] Schmidt, M.; Otto, A.; Kägeler, C.; Geiger, M.: Analysis of YAG Laser Lap-Welding of zinc coated steel sheets. CIRP Annals, E, 57/1/2008, P.213.
[5] Kaplan, A. F. H.: Keyhole surface waves during 1 µm-laser welding and resulting local absorptivity modulation. In: IIW Annual Assembly, Com IV, Denver, 2012.
[6] Klein, T; Vicanek, M.; Kroos, J; Decker, I.; Simon, G. (1994) Oscillations of the keyhole in penetration laser beam welding, J. Phys. D: Appl. Phys. 27 2023-2030.
[7] Boley, M.; Webster, P.; Heider, A.; Weber, R.; Graf, T.: Investigating the keyhole behavior by using x-ray and optical depth measurement techniques. In: In: Proceeding of 33nd International Congress on Applications of Lasers and Electro-Optics (ICALEO-2014), LIA Congress Proceeding. Paper 602.
[8] Berger, P.; Hügel, H.; Graf, T.: Understanding pore formation in laser beam welding. In: Physics Procedia 12 (2011) 241-247, World of Photonics Congress, 2011, Munich, Germany.
[9] Berger, P.; Hügel, H.; Graf, T.: Understanding pore formation in laser beam welding. In: Lasers in Manufacturing (LIM 2011), Physics Procedia 12, Elsevier Amsterdam (2011) 241-247.
[10] Gao, J.; Qin, G.; Yang, J.; He, J.; Zhang, T.; Wu, C.: Image processing of weld pool and keyhole in Nd:YAG laser welding of

stainless steel based on visual sensing. Trans. Nonferrous Met. Soc. China 21(2011) 423-428.
[11] Katayama, S.; Kawahito, Y.; Mizutani, M.: Plume behaviour and melt flows during laser and hybrid welding. In: Proceeding of the 4th International WLT-Conference on Lasers in Manufacturing 2007, Munich, 2007.
[12] Zhang, Y.; Chen, G.; Wei, H.; Zhang, J.: A novel „sandwich“ method for observation of the keyhole in deep penetration laser welding. In: Optics and Lasers in Engineering 46 (2008) 133-139, 2007.
[13] Geiger, M.; Kägeler, C.; Schmidt, M. (2008) High-power laser welding of contaminated steel sheets. In: Proc. Eng. Res. Devel. (2008) 2:235-240.
[14] Hoffman, J.; Szymanski, Z.; Jakubowski, J.; Kolasa, A. (2002) Analysis of acoustic and optical signals used as a basis for controlling laser-welding processes, in Welding International 2002 16 (1) 18-25.
[15] Fabbro, R.; Slimani S.; Coste F.; Briand F.; Dlubak B.; Loisel G. (2006) Analysis of basic processes inside the keyhole during deep penetration Nd:YAG cw laser welding, in Proceeding of the 25th International Congress on Applications of Lasers & Electro-Optics (ICALEO-2006) Laser Materials Processing Conference, Paper 101.
[16] Volpp, J.; Freimann, D. (2013) Indirect measurement of keyhole pressure oscillations during laser deep penetration welding. In: Proceeding of 32nd International Congress on Applications of Lasers and Electro-Optics (ICALEO-2013), LIA Congress Proceeding. Paper 1301, 334-340.
[17] Solana, P.; Ocana, J.L.: A mathematical model for penetration laser welding as a free-boundary problem. In: J. Phys. D: Appl. Phys. 30 (1997) 1300-1313.
[18] Pitz, I.; Otto, A.; Schmidt, M.: Accelerated simulation of laser beam forming by means of moving meshes. International Workshop on Thermal Forming and Welding Distortion (IWOTE), Bremen, April 06-07, 2011.
[19] Otto, A.; Koch, H.; Leitz, K.H., Schmidt, M. (2011) Numerical simulations – A versatile approach for better understanding dynamics in laser material processing, in Physics Procedia 12 (2011) 11-20, World of Photonics Congress, 2011, Munich, Germany.
[20] Klein, T.; Vicanek, M.; Simon, G.: Forced oscillations of the keyhole in penetration laser beam welding. In: J. Phys. D: Appl. Phys. 29 (1996) 322-332.
[21] Volpp, J.; Vollertsen, F. (2013) Analytical modeling of the keyhole including multiple reflections for analysis of the influence of different laser intensity distributions on keyhole geometry. In: Lasers in Manufacturing (LIM 2013), Physics Procedia 41, eds.: C. Emmelmann, M.F. Zaeh, T. Graf, M. Schmidt. Elsevier Amsterdam (2013) 453-461.
[22] Volpp, J.; Vollertsen, F.: Keyhole oscillations during laser deep penetration welding at different spatial laser intensity distributions. In: Proceeding of 33nd International Congress on Applications of Lasers and Electro-Optics (ICALEO-2014), LIA Congress Proceeding. Paper 601.
[23] Volpp, J.; Vollertsen, F.: Modeling keyhole oscillations during laser deep penetration welding at different spatial laser intensity distributions. In: Prod. Eng. Res. Devel. (2015) 9:167-178.
[24] Pleteit, H. (2001) Analyse und Modellierung der Keyhole-Dynamik beim Laserstrahlschweißen von Aluminiumlegierungen. Bremen, Univ., Diss., 2001. (in German)